Electronic supplementary information

A Versatile Biomimetic Multienzyme Cascade Nanoplatform Based on Boronic Acid-Modified Metal-Organic Framework for Colorimetric Biosensing

Hao Shen*, Haimei Shi, Bin Feng, Chuanfan Ding, and Shaoning Yu*

Key Laboratory of Advanced Mass Spectrometry and Molecular Analysis of Zhejiang Province, Institute of Mass Spectrometry, School of Material Science and Chemical Engineering, Ningbo University, Ningbo, Zhejiang 315211, China.

*Corresponding authors.

Email:

shenhao@nbu.edu.cn (for H. S.)

yushaoning@nbu.edu.cn (for S. Y.)

Experimental section

Characterization

The morphological characteristics of the synthetic materials were observed by transmission electron microscopy (TEM; JEM-2010HR, Tokyo, Japan) and scanning electron microscopy (SEM; Zeiss Supera55, Oberkochen, Germany). X-ray diffraction (XRD) patterns were investigated using an X-ray diffractometer (Bruker D8 Advance, Karlsruhe, Germany). The fluorescence measurements were confirmed by confocal laser scanning microscopy (CLSM; Leica SP8 X, Buffalo Grove, USA). Fourier-transform infrared (FT-IR) spectra were obtained by an infrared spectrometer (Thermo Fisher Nicolet iS20, Waltham, USA). Specific surface area was determined and pore volume and size analyzed using the Brunauer-Emmett-Teller (BET) and Barrett-Joyner-Halenda (BJH) methods, respectively, on a TR2 Star 3020 Surface Area & Pore Size Analyzer (Micromeritics, Norcross, USA). X-ray photoelectron spectra (XPS) were recorded on an X-ray photoelectron spectrometer (Thermo VG Escalab 250, Waltham, USA) at a pressure of approximately 2×10^{-9} Pa with Al Kα X-rays as the excitation source. Inductively coupled plasma mass spectrometry (ICP-MS) system (Agilent 7700s, USA) were employed to evaluate elemental constituent contents of the samples. ^{11}B NMR spectra were recorded on a Varian INOVA500NB spectrometer. Enzymatic assays were carried out using a UV-Vis spectrophotometer (Hitachi UH5300, Tokyo, Japan).

TAC assay

TAC assays of commercial beverages and health products (vitamin water, green tea, orange juice, tablet, and milk powder) were carried out using AA as a typical model. First, the selectivity of the colorimetric sensor was investigated using metal ions (Mg^{2+}, Na^{+}, and Cu^{2+}, 5 mM), amino acid (glutamic acid, 5 mM), carbohydrates (glucose, lactose, and sucrose, 5 mM), and bovine serum albumin (BSA, 1 mg/mL). To pre-treat the real samples, beverages were filtered through a 0.45-μm filter and kept in the dark at 4°C. Solid tablet/powder was ground, dissolved in acetate buffer (0.2 M, pH 4), filtered through a 0.45-μm filter, and kept in the dark at 4°C as well. The concentrations of these samples were then diluted to avoid exceeding the linear range of AA detection. TAC assays were evaluated under the same conditions as AA detection but used the real sample to replace AA.

The absorbance of ox-TMB was brought into the standard curve and converted to the millimolar equivalents of AA. Next, the value of TAC was obtained through absorbance conversion and multiplied by the dilution factor. Finally, AA L^{-1} was used as a unit to indicate the TAC content in the sample.

GSH detection in real samples

First, eye drops were diluted 100 times with acetate buffer (0.2 M, pH 4), filtered through a 0.45-μm filter, and then stored in the dark at 4°C. Chewable tablets and whitening powder (100 mg of each) were ground, dissolved in acetate buffer (0.2 M, pH 3, 100 mL), filtered through a 0.45-μm filter, and stored in the dark at 4°C. The GSH levels in these samples were evaluated under the same conditions as GSH detection but used the real sample to replace GSH. The value for GSH was obtained using the standard curve and multiplied by the dilution factor.

Fluorescence labeling of enzymes

FITC and RhB labeling were based on the conjugation of the amino of lysine residues of enzymes and the thiocarbmide of fluorescent dyes. Briefly, 20 mg of enzyme was dispersed into 10 mL carbonate buffer solution (0.5 M, pH 9.0) and 1 mg of fluorescence dye (FITC or RhB) added. The mixed solution was then stirred for 12 h in the dark. Finally, the dye-labeled enzymes were obtained by performing ultrafiltration three times to remove excess reaction reagents and salts.

Effect of catalase on cascade reaction

Sarcosine (800 μL, 5 mM), TMB (100 μL, 5 mM), and MES buffer (90 μL, 50 mM, pH 6) were added into the SOX@MIL-100(Fe)-BA suspension (10 μL, 1 mg mL^{-1}) and various concentrations of catalase (1, 2.5, 5, 10 and 25 μM). The mixture was reacted at 40°C for 15 min and centrifuged to detect the absorbance of the supernatant at 652 nm using UV-Vis.

Fluorescence characterization of the cascade nanoplatform

The fluorescence spectra of free SOX suspension (0.25 mg mL^{-1}) and SOX@MIL-100(Fe)-BA suspension (0.35 mg mL^{-1}) were recorded at room temperature using a spectrofluorometer with an excitation wavelength at 280 nm.

Kinetic investigation of SOX@MIL-100(Fe)-BA

SOX@MIL-100(Fe)-BA suspension (10 μL, 1 mg mL^{-1}), TMB (100 μL, 5 mM), and MES buffer (90 μL, 50 mM, pH 6) were added into different concentrations of sarcosine (800 μL, 0.5, 0.625, 1, 2, 4 and 8 mM) to make up the final volume to 1 mL. The reaction was carried out at 40°C for 15 min and centrifuged to detect the absorbance of the supernatant at 652 nm using UV-Vis. The steady-state kinetics of free enzymes were the same as the above steps.

Colorimetric sarcosine/ACh detection in real samples

To establish the standard curve for sarcosine determination, the SOX@MIL-100(Fe)-BA stock solution (10 μL, 1 mg/mL) was added to MES buffer solution (50 mM, pH 6) containing 1 mM TMB and various concentrations of sarcosine (1, 2, 5, 10, 25, 50, 75, 100, 150, 200, and 250 μM). The above mixture was reacted for 15 min at 40°C and the absorbance of the supernatant recorded at 652 nm. To investigate the selectivity of the colorimetric sensor, sarcosine (100 μM), alanine, aspartic acid, glycine, histidine, lysine, serine, tyrosine, and uric acid (1 mM for each) were added in MES buffer containing 1 mM TMB. The solutions were then mixed with SOX@MIL-100(Fe)-BA for 15 min at 40°C. The absorbance of the supernatant was detected at 652 nm. For sarcosine detection in urine, samples were centrifuged (12 000 rpm) for 15 min and the sediment removed. SOX@MIL-100(Fe)-BA stock solution (10 μL, 1 mg/mL) was mixed with diluted urine samples (800 μL) and TMB solution (1 mM, 190 μL). The above mixture was reacted for 15 min at 40°C and the absorbance of the supernatant recorded at 652 nm. A certain amount of sarcosine was then added to the urine to obtain spiked samples. The sarcosine levels in these spiked samples were detected via the above method.

The evaluation of ACh concentrations in real samples by AChE/ChOx@MIL-100(Fe)-BA was similar, except that the substrate ACh was used instead of sarcosine. The milk samples were diluted, mixed with acetonitrile, and centrifuged to remove the proteins.

Table S1 Kinetic parameters of MIL-100(Fe), HRP, and other reported nanozymes.

Catalyst	K_m (mM)		V_{max} (10^{-8} M/s)		Reference
	H_2O_2	TMB	H_2O_2	TMB	
HRP	3.7	0.434	8.71	10	[1]
Fe-MIL-88-NH_2	2.06	0.284	7.04	10.47	[2]
MIL-53(Fe)	0.04	1.08	11.16	52.68	[3]
MIL-100(Fe)-BA	0.771	0.467	1.73	2.51	This work

Table S2 Performance of different sensing systems in AA detection.

Catalyst	Method	Linear range (μM)	LOD (μM)	Ref.
MIL-53(Fe)	Colorimetric	28.6-190.5	15	[3]
MIL-68/MIL-100	Colorimetric	30-485	6	[4]
SNC-900	Colorimetric	100-5000	80	[5]
Cu NPs@C	Colorimetric	10-1000	1.41	[6]
CoOOH-modified TPNPs	Fluorometric	1-20	0.17	[7]
Au/RGO	Electrochemical	240-1500	50	[8]
MIL-100(Fe)-BA	Colorimetric	5-750	0.94	This work

Table S3 Added-standard recovery results for determination of AA in real samples.

Sample	Determined by HPLC (mM)	Proposed method (mM)	Added (mM)	Found (mM)	Recovery (%)	RSD (%, n=3)
Vitamin water	0.66	0.57	0.50	1.11	108.0	1.9
Green tea	0.15	0.18	0.50	0.64	92.0	1.5
Orange juice	0.48	0.46	0.50	0.94	96.0	2.3
Tablet	1.29	1.42	0.50	1.94	104.0	4.6
Milk powder	1.14	1.08	0.50	1.61	106.0	3.9

Table S4 Added-standard recovery results for determination of GSH in real samples.

Sample	Determined by HPLC (μM)	Proposed method (μM)	Added (μM)	Found (μM)	Recovery (%)	RSD (%, n=3)
Chewable tablets	18.6	18.1	5.0	22.9	96.0	2.7
			15.0	33.3	101.3	1.6
Eye drops	9.1	9.3	5.00	14.7	108.0	1.8
			15.00	24.9	104.0	1.7
Whitening powder	5.8	5.5	5.00	10.8	106.0	2.4
			15.00	20.0	96.7	2.9

Table S5 Performance of different sensing systems in sarcosine detection.

Catalyst	Method	Linear range (μM)	LOD (μM)	Ref.
TCPP-Pt/SOX@HMUiO	Fluorometric	0-100	2.1	[9]
silica-R5$_2$-mCh-mSOx-R5-6H	Fluorometric	2.5-10	-	[10]
$CuInS_2$/NiO/ITO	Electrochemical	10-1000	-	[11]
FA-PMo_4V_8	Colorimetric	0.2-500	0.311	[12]
Pd NPs	Colorimetric	0.01-50	5×10^{-3}	[13]
SOX@MIL-100(Fe)-BA	Colorimetric	1-250	0.26	This work

Table S6 The intra-run and inter-run precision of SOX@MIL-100(Fe)-BA for colorimetric detection of sarcosine.

Sarcosine (μM)	Intra-run		Inter-run	
	Mean ± SD	CV (%, n = 6)	Mean ± SD	CV (%, n = 6)
1.00	1.06 ± 0.02	4.62	1.08 ± 0.02	6.41
5.00	5.32 ± 0.08	6.77	5.46 ± 0.13	2.58
50.00	50.16 ± 0.44	5.09	50.24 ± 0.37	3.96
100.00	97.84 ± 0.16	3.56	98.02 ± 0.26	6.56

Table S7 Comparison of biosensors for the detection of ACh.

Catalyst	Method	Linear range (μM)	LOD (μM)	Ref.
CdTe QDs	Fluorometric	10-500	10	[14]
MWCNT-AuNP-(PDDA-AChE)$_2$/Pt	Electrochemical	5-400	1	[15]
CdS NCs	Electrochemiluminescence	3.3-332	1.7	[16]
Cu-N-C SAzymes	Colorimetric	10-8000	1.24	[17]
AChE/ChOx@MIL-100(Fe)-BA	Colorimetric	6-9600	1.18	This work

Table S8 Detection precision of the AChE/ChOx@MIL-100(Fe)-BA-based assay system for the determination of ACh in milk samples.

Sample	Added value (μM)	Measured value (μM)	SD	CV (%)	Recovery (%)
1	10	9.81	0.36	3.67	98.1
2	50	53.44	1.54	2.88	106.9
3	100	102.86	2.29	2.23	102.9
4	1000	978.24	18.68	1.91	97.8

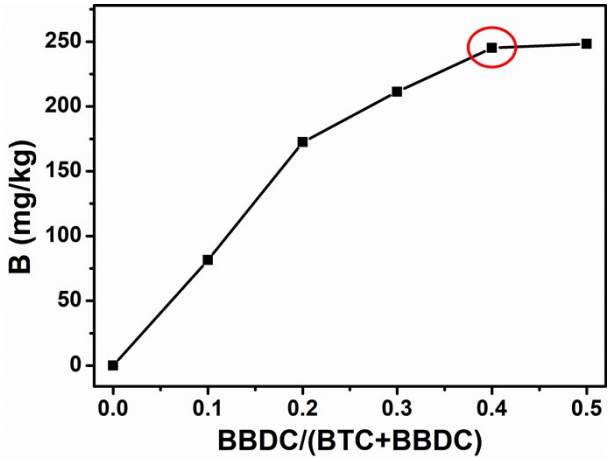

Fig. S1 The effect of BBDC content in the initial reactant mixture on the amount of boron in MIL-100(Fe)-BA.

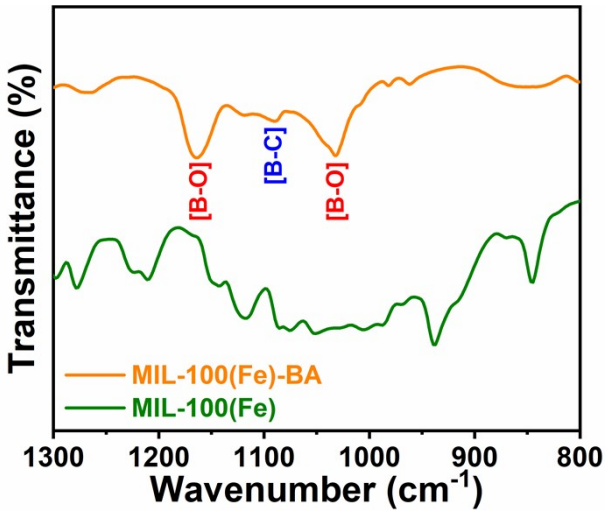

Fig. S2 FT-IR analysis of MIL-100(Fe)-BA and MIL-100(Fe).

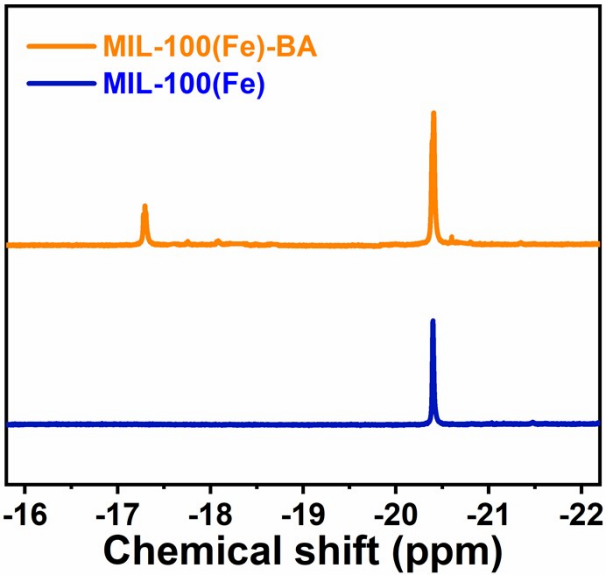

Fig. S3 ^{11}B NMR spectra of digestion products of MIL-100(Fe)-BA and MIL-100(Fe).

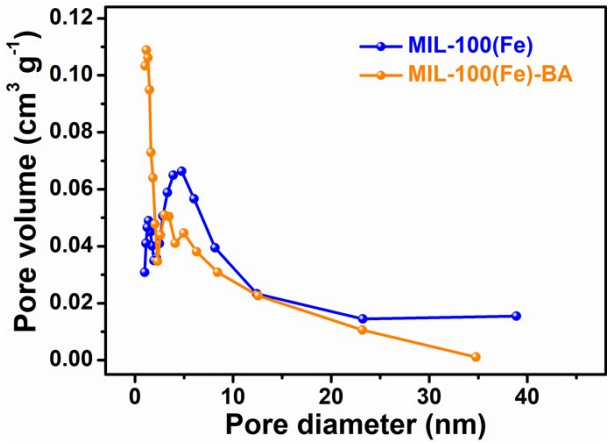

Fig. S4 Pore size distribution of MIL-100(Fe) and MIL-100(Fe)-BA.

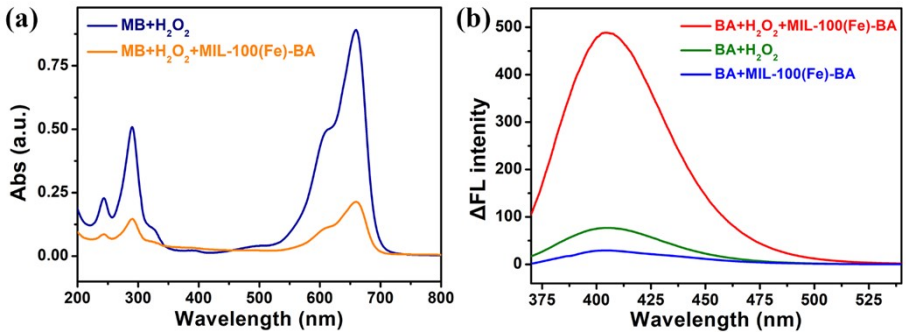

Fig. S5 (a) Absorbance spectra of MB before and after addition of MIL-100(Fe)-BA. (b) Fluorescence spectra in various reaction systems.

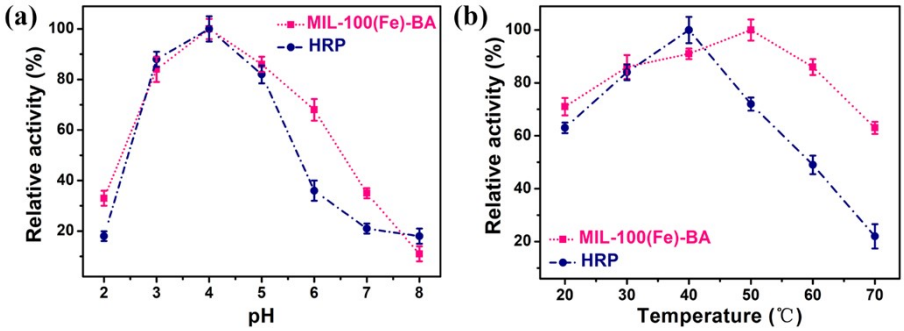

Fig. S6 (a) Effect of pH and (b) temperature on the biomimetic activity of MIL-100(Fe)-BA.

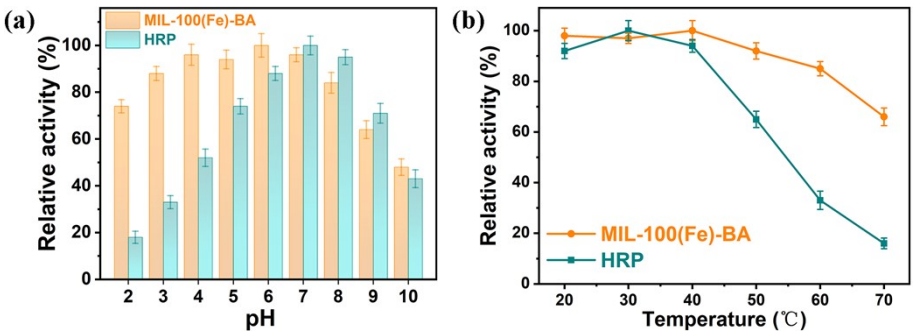

Fig. S7 The pH (a) and thermal (b) stability of MIL-100(Fe)-BA.

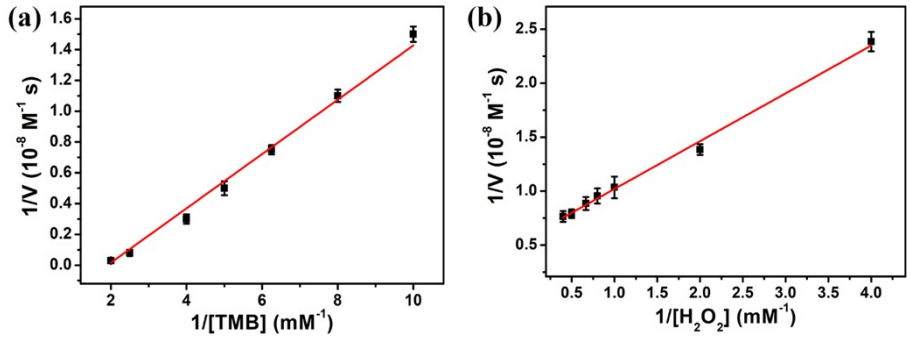

Fig. S8 Lineweaver Burk double-reciprocal model for MIL-100(Fe)-BA towards TMB (a) and H_2O_2 (b).

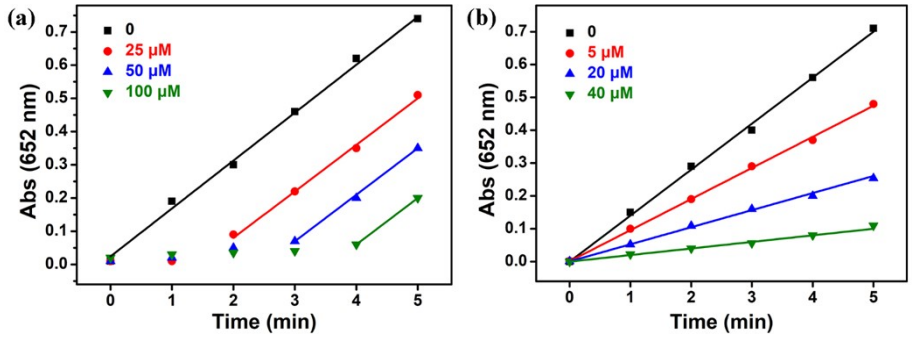

Fig. S9 (a) Concentration-dependent quenching effects of AA on the peroxidase-like activity of MIL-100(Fe)-BA. (b) Concentration-dependent quenching effects of GSH on the oxidase-like activity of MIL-100(Fe)-BA.

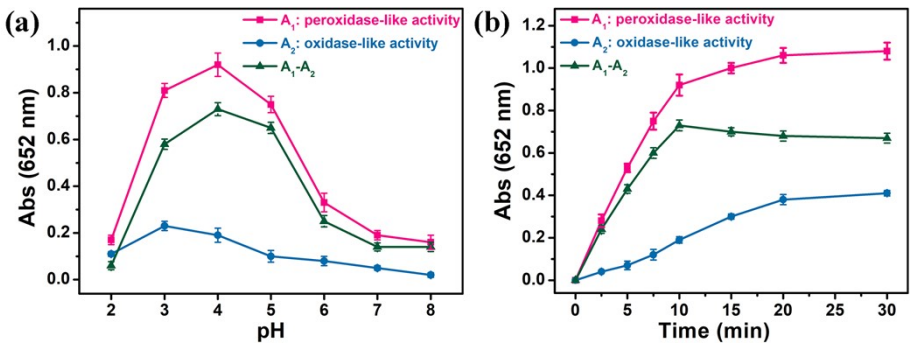

Fig. S10 Optimization of pH (a) and reaction time (b) of MIL-100(Fe)-BA with dual enzyme catalytic activity.

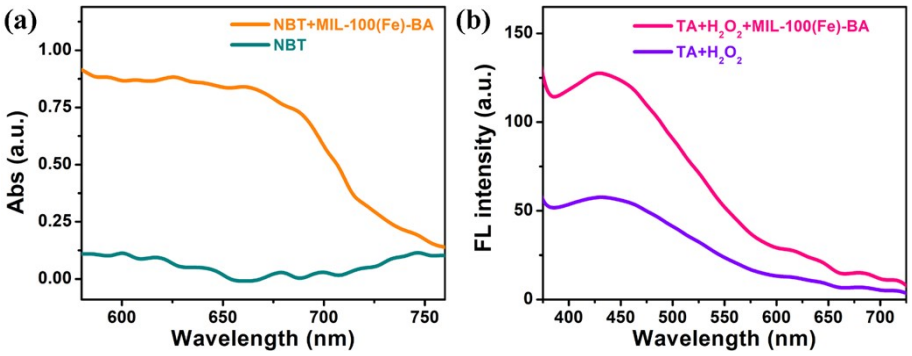

Fig. S11 (a) The UV-vis spectra of nitro blue tetrazolium (NBT) and the reaction mixture of MIL-100(Fe)-BA-catalyzed reduction of NBT in DMSO. (b) Fluorescence spectra of reaction solutions containing MIL-100(Fe)-BA, H_2O_2, and terephthalic acid (TA).

NBT is a compound which can react with the superoxide anion radical ($O_2^{\cdot-}$) and then can be reduced to formazan with maximum absorbance at 680 nm.[18] It is known that the superoxide anion is stable in DMSO. As shown in Fig. S11a, The emergence of the absorption peak of the reduced NBT suggested the generation of the superoxide anion in the reaction. Furthermore, TA was here selected as the fluorescent probe for tracking hydroxyl radicals (·OH) to produce 2-hydroxy terephthalic acid with an emission peak around 425 nm.[19] The result in Fig. 11b confirms the production of hydroxyl radicals. Hence, both the superoxide anion and the hydroxyl radical could be active oxygen species in the present catalytic system.

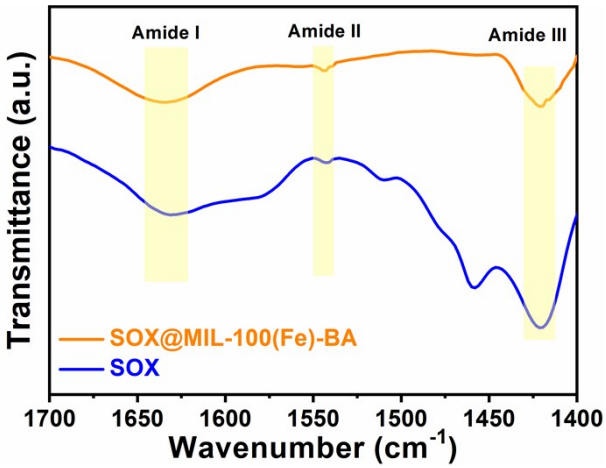

Fig. S12 FTIR spectra of SOX and SOX@MIL-100(Fe)-BA nanocomposite.

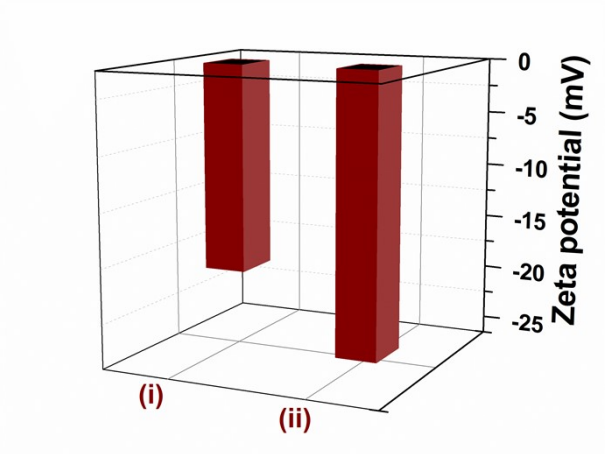

Fig. S13 Zeta potentials of MIL-100(Fe)-BA (i) and MIL-100(Fe) (ii).

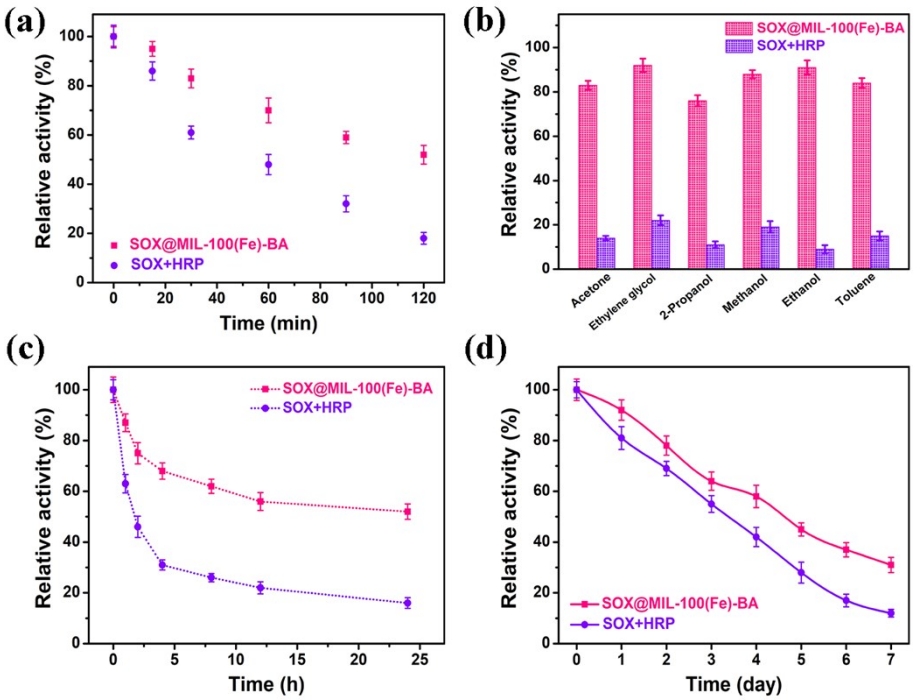

Fig. S14 Stability of SOX@MIL-100(Fe)-BA compared with and free enzymes at the same enzyme concentration: (a) heat endurance at 60°C; (b) tolerance towards different organic solvents; (c) relative activity in high salt ion concentration solution (4 M of sodium phosphate); (d) prolonged immersion under 40 °C.

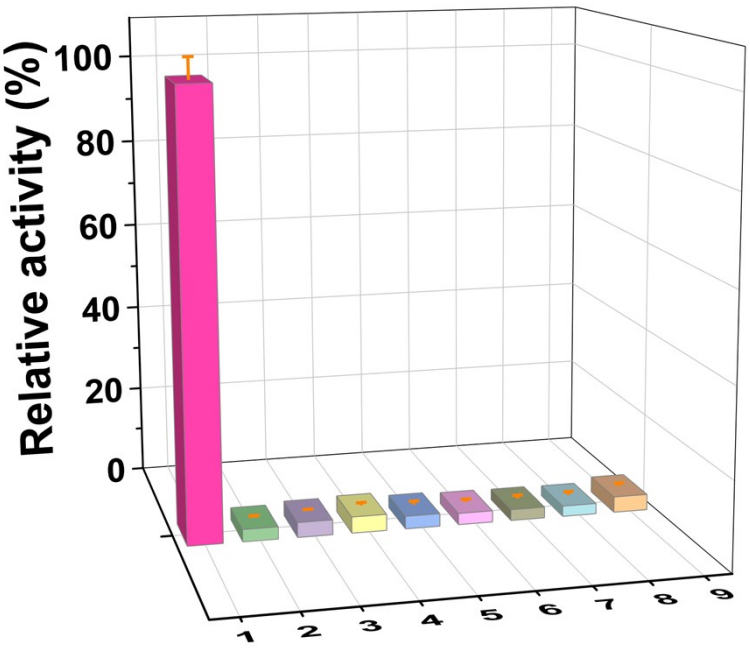

Fig. S15 The absorbance of different substrates in the sarcosine assay, which are (1) sarcosine, (2) glucose, (3) ascorbic acid, (4) urea, (5) Na^+, (6) Ca^{2+}, (7) Cu^{2+}, (8) K^+ and (9) NH_4^+, respectively.

REFERENCES

[1] J. Wang, Y. Hu, Q. Zhou, L. Hu, W. Fu and Y. Wang, ACS Appl. Mater. Inter., 2019, 11, 44466-44473.

[2] Y. Liu, X. Zhao, X. Yang and Y. Li, Analyst, 2013, 138, 4526-4531.

[3] L. Ai, L. Li, C. Zhang, J. Fu and J. Jiang, Chem. Eur. J., 2013, 19, 15105-15108.

[4] J. Zhang, H. Zhang, Z. Du, X. Wang, S. Yu and H Jiang, Chem. Commun., 2014, 50, 1092-1094.

[5] Y. Chen, L. Jiao, H. Yan, W. Xu, Y. Wu, H. Wang, W. Gu and C. Zhu, Anal. Chem., 2020, 92, 13518-13524.

[6] H. Tan, C. Ma, L. Gao, Q. Li, Y. Song, F. Xu, T. Wang and L. Wang, Chem. Eur. J., 2014, 20, 16377-16383.

[7] H. Meng, X. Zhang, C. Yang, H. Kuai, G. Mao, L. Gong, W. Zhang, S. Feng and J. Chang, Anal. Chem., 2016, 88, 6057-6063.

[8] C. Wang, J. Du, H. Wang, C. Zou, F. Jiang, P. Yang and Y. Du, Sens. Actuators B: Chem., 2014, 204, 302-309.

[9] L. Zhao, J. Yang, M. Gong, K. Li and J. Gu, J. Am. Chem. Soc., 2021, 143, 15145-15151.

[10] C. J. Henderson, E. Pumford, D. J. Seevaratnam, R. Daly and E. A. H. Hall, Biomaterials, 2019, 193, 58-70.

[11] X. Jiang, L. Zhang, Y. Liu, X. Yu, Y. Liang, P. Qu, W. Zhao, J. Xu and H. Chen, Biosens. Bioelectron., 2018, 107, 230-236.

[12] B. Mbage, Y. Li, H. Si, X. Zhang, Y. Li, X. Wang, A. Salah and K. Zhang, Sens. Actuators B: Chem., 2020, 304, 127429.

[13] J. Lan, W. Xu, Q. Wan, X. Zhang, J. Lin, J. Chen and J. Chen, Anal. Chim. Acta, 2014, 825, 63-68.

[14] Z. Chen, X. Ren, X. Meng, D. Chen, C. Yan, J. Ren, Y. Yuan and F. Tang, Biosens. Bioelectron., 2011, 28, 50-55.

[15] S. Hou, Z. Ou, Q. Chen and B. Wu, Biosens. Bioelectron., 2012, 33, 44-49.

[16] X.-F. Wang, Y. Zhou, J.-J. Xu and H.-Y. Chen, Adv. Funct. Mater., 2009, 19, 1444-1450.

[17] Y. Wu, J. Wu, L. Jiao, W. Xu, H. Wang, X. Wei, W. Gu, G. Ren, N. Zhang, Q. Zhang, L. Huang, L. Gu and C. Zhu, Anal. Chem., 2020, 92, 3373-3379.

[18] S. Cai, C. Qi, Y. Li, Q. Han, R. Yang and C. Wang, J. Mater. Chem. B, 2016, 4, 1869-1877.

[19] X. Liang and L. Han, Adv. Funct. Mater., 2020, 30, 2001933.